ELSEVIER

Pattern Recognition Letters 20 (1999) 1389–1396

Pattern Recognition Letters

www.elsevier.nl/locate/patrec

An evolutionary system for recognition and tracking of synoptic-scale storm systems

J.A. Parikh [a,*], J.S. DaPonte [a], J.N. Vitale [a], G. Tselioudis [b]

[a] *Computer Science Department, Southern Connecticut State University, New Haven, Connecticut, CT 06515, USA*

[b] *Columbia University and NASA Goddard Institute for Space Studies, New York, NY 10025, USA*

Abstract

An evolutionary system was developed for generation of complete tracks of northern midlatitude synoptic-scale storm systems based on optical flow and cloud motion analyses of global satellite-based datasets produced by the International Satellite Cloud Climatology Project (ISCCP). The tracking results were compared with low sea level pressure anomaly (SLPA) tracks obtained from the NASA Goddard Institute for Space Studies (GISS). The SLPA tracks were produced at GISS by analysis of meteorological, ground-based National Center for Environmental Prediction (NCEP) datasets. Results from the evolutionary system were also compared with results from using (a) the *k*-nearest neighbor rule (*k*-NN) and (b) self-organizing maps (SOM) to determine correspondences between consecutive locations within a track. The consistency of our evolutionary storm tracking results with the behavior of the low sea level pressure anomaly tracks, the ability of our evolutionary system to generate and evaluate complete tracks, and the close comparison between the results obtained by the evolutionary, *k*-NN, and SOM analyses of the ISCCP-derived datasets at tracking steps in which proximity or optical flow information sufficed to determine movement, demonstrate the applicability and the potential of evolutionary systems for tracking midlatitude storm systems through low-resolution ISCCP cloud product datasets.

Keywords: Cloud tracking; Evolutionary computation; Optical flow; Self-organizing maps; *k*-nearest neighbor analysis

1. Introduction

Clouds are a major source of uncertainty in our attempts to use models to predict future climate change. In the middle latitudes, clouds are primarily organized along storm systems that travel down the path of the jet stream and constitute the main weather makers in the region. The cloud properties of individual storms have been examined in several meteorological studies; the structure and movement of the overall midlatitude cloud field, however, have not been investigated in detail, partly due to the lack of data with sufficient time and space resolution. Knowledge of the properties of the midlatitude cloud field is very important in the study of climate change, since in a warmer climate, changes in clouds can produce strong feedbacks that must be correctly resolved by climate models. The advent of a global satellite cloud climatology (Rossow and Schiffer, 1991) gives us the opportunity to examine in long time and space scales the structure and movements of the midlatitude cloud field.

* Corresponding author.

E-mail addresses: parikh@scsu.ctstateu.edu (J.A. Parikh), ccgxt@giss.nasa.gov (G. Tselioudis)

0167-8655/99/$ - see front matter
PII: S 0 1 6 7 - 8 6 5 5 (9 9) 0 0 1 1 0 - 5

This study uses satellite-derived cloud property data to track midlatitude storm systems. The presence of high-top, optically thick clouds is used here as an initial indicator of a storm system, based on the results of the paper by Tselioudis et al. (1999). The objective of the study is to derive methods that provide a comprehensive description of the large-scale structure and movement of the midlatitude cloud field, so that in the future we will be able to investigate the seasonal and interannual variation of those large-scale cloud field properties. The results of this investigation will provide climate modelers with a valuable tool to evaluate their model simulations and will give important information on potential changes in midlatitude cloud properties with climate change.

Previous work in tracking objects has included a variety of analytical approaches. Arnaud et al. (1992) developed an automatic system for tracking African convective systems which resulted in generating climatological statistics to describe the time evolution of the convective systems. Their method was primarily based on cloud labeling and the identification of intersections between successive images. Endlich and Wolf (1981) investigated feature tracking by using pattern recognition algorithms. Silver and Wang (1997) used spatial overlaps to determine the evolutionary history of objects extracted from computational fluid dynamics datasets. The distance between the centers of regions and differences in region areas were the basis for a cost function used to determine the correspondence of regions from one frame to another in a method developed by Bolla et al. (1997). Lane et al. (1998) used optical flow calculations and tracking trees to track moving objects in sequences of sector-scan sonar images. A genetic algorithm approach based on template matching and discriminant strength was used by Carbonaro and Singaretti (1997) to track video-recorded image sequences. Parikh et al. (1997, 1998) outlined a methodology for using evolutionary techniques that involve neural networks and genetic algorithms to achieve temporal classification of cloud systems as well as automatic techniques for identifying and tracking synoptic-scale storm systems (Parikh et al., 1999).

An excellent review of techniques and difficulties associated with determination of non-rigid or evolving pattern movement in environmental satellite imagery can be found in (Wu, 1995). Wu developed a correlation and relaxation-labeling framework for computation of optical flow, applied his technique to determination of cloud motion in infrared images, and contrasted his technique to classical techniques such as template matching and gradient-based optical flow techniques. Several general optical flow techniques that are not necessarily oriented toward cloud motion are reviewed and compared by Barron et al. (1994). One of the region-based matching techniques, a technique developed by Anandan (1989), as described and implemented by Barron et al. (1994) was used in this study for computation of optical flow estimates.

The literature on genetic algorithms and evolutionary computation includes several examples of evolutionary systems that have been used for motion segmentation, robotic navigation and shortest path problems. Two evolutionary systems that are particularly analogous to our cloud tracking evolutionary system with respect to type of problem and evolutionary methodology are the Evolutionary Planner/Navigator (EP/N) system (Xiao et al., 1997) for robotic navigation and the multiresolution genetic algorithm (MGA) developed by Voicu and Myler (1998). Our evolutionary system seeds the search space with potentially good partial storm tracks in a manner similar to the way in which the Voicu and Myler cloning operator constructs and extends partial paths when searching for shortest paths in planar graphs. The approach of distinguishing and developing different evaluation functions for feasible and for infeasible paths was a technique that was used in both our system and in the EP/N robotic navigation system.

In this paper, we describe the preprocessing of datasets for our evolutionary system, our evolutionary methodology, and the results of comparing the output from our system with tracks produced from analyses of low sea level pressure anomalies (SLPA) and with tracks from correspondence-based analyses using (a) the *k*-nearest neighbor rule (*k*-NN) and (b) self-organizing maps (SOM).

Section 2 outlines the process of constructing time-sampled cloud optical thickness and cloud top pressure datasets from ISCCP datasets. The process of selecting candidate pixels and/or collections of pixels that could potentially be members of a storm track is explained in Section 3. Section 4 describes our *k*-NN and SOM correspondence-based approaches for determination of storm tracks. The details of our evolutionary methodology together with illustrative results are presented in Section 5. In Section 6 we conclude with a general discussion of results and suggestions for future research.

2. Construction of time-sampled datasets

From stage D1 ISCCP datasets for the first 12 days in April 1989, cloud optical thickness (TAU) and cloud top pressure (CTP) parameters were extracted. The D1 ISCCP datasets, which summarize and merge stage DX pixel-level results from several satellites, have a spatial resolution of 280 km and a temporal resolution of 3 h. The cloud top pressure and the cloud optical thickness equal-area datasets can be, and generally are, displayed and analyzed as images with 144 columns and a maximum of 72 rows in which values of data at latitudes north and south of the equator are repeated two or more times as needed to create an image with values at every 2.5° of latitude and 2.5° of longitude. In order to analyze the cloud structures within the northern midlatitudes from 30°N to 60°N, we extracted 28 rows of data which covered the latitudes from 0°N to 70°N. With the exception of data missing due to failure of satellite coverage, cloud top pressure values, which are based on infrared (11 μm wavelength) observations of cloud top temperature, are typically available every 3 h. However, cloud optical thickness values, which are based on satellite observations in the visible spectrum (0.6 μm wavelength), are typically missing for over one-half of the globe (72 or more columns in the image) due to lack of reflected sunlight during night-time hours.

The importance of cloud optical thickness (TAU) values in the characterization of storm systems in the northern midlatitudes makes it imperative that this information be included in the analysis of cloud tracks associated with storm systems. In any given region of the globe, the maximum number of consecutive TAU values that could be reliably obtained during a 24 h period was three (corresponding to a period of about 9 h of daylight). Although our analysis could have been performed using the unprocessed TAU images, we decided, for purposes of simplification of optical flow feature extraction and identification of cloud structures associated with storm systems, to construct time-sampled TAU images.

A time-sampled TAU image consists of eight different longitude intervals of TAU data sampled from eight consecutive three-hourly ISCCP datasets. Neighboring longitude intervals (groups of columns) in a time-sampled image contain TAU values that are separated in time by 3 h. At any given spatial location within a sequence of time-sampled TAU images, consecutive TAU values at the same location will be actual TAU values extracted from ISCCP datasets separated in time by either 3 or 15 h. Using the time-sampled TAU values for tracking meant that the tracks that were generated consisted of two steps separated by 3 h followed by one 15 h step. For each time-sampled TAU image, a corresponding time-sampled CTP image was constructed so that at any given spatial location the TAU and CTP information in the corresponding images came from the same time frame.

3. Identification of candidate tracking events

A synoptic-scale storm system is characterized by long track duration and existence within the track of one or more events (regions of interest) that satisfy the ISCCP radiometric cloud classification criteria for deep convection. In order to identify the start of a track and other possible tracking events along a track, the cloud optical thickness (TAU) data and the cloud top pressure (CTP) data in the corresponding time-sampled images were thresholded at values corresponding to 23 and 440 mb, respectively, which demarcate deep convective cloud systems as defined in the ISCCP classification scheme. Regions consisting of three or more distinct connected points that met the deep convective cloud system criteria were considered as possible candidates for the beginning of a storm track. In order to confirm that a region represented the beginning of a storm track, a search had to be conducted within the previous time-sampled images to confirm that there were no possible predecessors.

Coupled with the identification of deep convective cloud systems, a multi-threshold technique was applied to the time-sampled TAU images to extract candidate tracking events that might appear along a storm track after the initial region of tracking events had been identified. The TAU images were thresholded and labeled connected components extracted for three different threshold levels. The first level corresponded to the TAU criteria of 23 and above for cloud optical thickness for deep convective systems. The second and third threshold levels corresponded to TAU criteria of 13.5 and 9.4, respectively. For all three threshold levels, in each of the connected components, all points that had a value of TAU that was equal to the maximum TAU value within that component were extracted and added to the pool of candidate tracking events.

4. Feature extraction

A binary image was formed for each time period consisting of candidate tracking events. Each image consisted of only two gray levels, 0 and 255. From these sequences of binary images, optical flow estimates for each pixel in every time frame were extracted using the technique developed by Anandan (1989) as implemented by Barron et al. (1994). For each pixel in the candidate tracking event images, other features that were extracted included the location of the tracking event itself (row and column coordinates), location in the next frame of the nearest point to the east allowing westward movement of at most one pixel, and location in the next frame of the closest point. For the k-nearest neighbor analysis, the TAU values from the time-sampled images were retained and formed one of the features in the input datasets.

5. Track generation by correspondence determination

Two techniques for determination of the best corresponding tracking event in the next image were applied to input datasets. The input datasets contained expected projected locations in the next image of the current tracking location based on optical flow estimates and on nearest projected tracking event to the east calculations. The first technique, the k-nearest neighbor rule, included within training and test datasets TAU values and analyzed exclusively tracking events whose TAU values met the deep convective system TAU threshold level of greater than or equal to 23. The second technique, self-organizing neural networks or maps, was based on projections and included candidate tracking events from all three threshold levels.

5.1. k-nearest neighbor (k-NN) analysis)

For each time frame in a given sequence of n time steps from time t_2 to time t_n, the k-nearest neighbor classifier with $k = 1$ was applied to the input datasets described above using the input dataset from the previous time step as the calibration dataset. In the test dataset, features representing projected locations were replaced by the actual location of the candidate tracking event. Class categories were defined as the component labels associated with the highest threshold value (TAU = 23) from the dataset at the previous time step. Output for a dataset for time t_i consisted of a point-by-point listing of points labeled with class categories that were component labels associated with components from time t_{i-1}. Each individual point in a connected component c_i for a dataset for time t_i thus had a component label l_{c_i} associated with time t_i and a component label $l_{c_{i-1}}$ associated with time t_{i-1}. The location of the track at time t_i was defined as the location of the tracking event with the maximal TAU value within the component labeled l_{c_i}. Thus, through a process of progressive training and testing cycles for each time step, tracks were generated proceeding from corresponding connected components.

5.2. Self-organizing map (SOM) analysis

The self-organizing map neural network clusters items in the input dataset into categories of similar objects by creating a two-dimensional feature map (layer of processing elements or nodes). With each node in the feature map is associated a reference or codebook vector in higher-dimensional space. An input vector is mapped onto the feature node whose reference or codebook vector provides the best match to the input vector. Reference or codebook vectors are obtained after a given number of training iterations have been performed in order to stabilize the SOM.

The Self-Organizing Map Program Package SOM_PAK (Kohonen et al., 1995) developed by the SOM founder, Teuvo Kohonen, and his colleagues at the Helsinki University of Technology was used to implement neural network analysis of tracking event correspondences in this study. The feature vectors used as input to the SOM consisted of the row and column coordinates in the next consecutive frame of the optical flow projections and the row and column coordinates in the next consecutive frame of the nearest point to the east projections. No TAU features were included. The tracking events included all tracking events isolated at all three threshold levels which was different from the number of tracking events processed by the k-NN analysis. Calibration labels consisted of connected component labels which were different for each of the threshold levels. The SOM architecture used was a 12×18 rectangular lattice. As in the k-NN analysis, the location features in the test sets were set identically equal to the actual coordinates of the location of the tracking event. Calculation of tracks then proceeded by determination of which, if any, of the calibrated units or component labels from a training run on the previous image corresponded to a given tracking event in the test set. Tracking always proceeded by looking for the component label at the highest or deep convective threshold level before examining tracking events that did not meet the deep convective system TAU criteria.

The steps in the implementation of the SOM network consisted of:

1. random initialization of the 12×18 rectangular feature map;
2. (phase 1 map training for 1000 iterations, using a neighborhood radius of 10 and a learning rate of 0.05;
3. phase 2 map training for 10000 iterations, using a neighborhood radius of three and a learning rate of 0.02;
4. calibration using the input dataset for time t_{i-1};
5. visualization using the dataset for time t_i.

Correspondences were obtained by determination of the component labels of the feature nodes and tracking was performed as described above as a result of the visualization and calibrations steps.

6. Track generation by evolutionary computation

Evolutionary systems use principles of evolution to optimize functions. In an evolutionary system, the coding of a chromosome or individual in a population must be defined, genetic operators for recombination, mutation and selection must be specified, and a fitness function for evaluation of each individual in the population and selection for recombination must be constructed. The system then continues to evolve new populations until some termination condition such as maximum number of iterations has been satisfied. At that time, the best individual or individuals in the population represent the solution to the optimization problem.

For our system, each individual in a population represented a track. A chromosome or individual consisted of n integers, where n represents the number of time-sampled images in the image sequence. The value of n for our experiments was 34 which corresponded to about a 12 day period. If a tracking event was found in an image at time i in the sequence as described above, then all integer values in the chromosome prior to the ith value were set to a no-event value such as -1. In each of the images, candidate tracking events were numbered consecutively starting at 1. The tracking number for the beginning of the track was then used as the only possible value for the integer at position i in the chromosome. The integer values for other positions j following position i could range from zero which represented the end of a track to the number of tracking events n_{t_j} in image j as the number of iterations increased. Initially only the value at position $i+1$ was allowed to vary.

Specialized application-specific mutation and crossover operators were defined for an initial period in the evolutionary process in order to seed the population or search space with good partial tracks. After every m iterations, where m was set to 20 for our experiments, mutation was specified to occur at the next position only. After the initial period passed, mutation could occur at any valid position. The crossover operator used was one-point crossover in order that good partial paths would not be disrupted. During the initial seeding period, crossover was restricted to the site of track extension. These specialized operators, in addition to a special routine for initialization of the population were added as customized operators into PGAPack, a parallel genetic algorithm library (Levine, 1996), which was used for our experiments.

The function to be optimized or minimized was the sum of all the distances or absolute values of deviations along the track from the best projections based on connected component correspondences for the lowest threshold level, optical flow projections, nearest point to the east projections and closest point projections. A flowchart of the procedure is given in Fig. 1. The component pair classes consisted of class labels for every pair of connected components in consecutive images, describing whether or not the relationship between the two components was (1) a direct correspondence, (2) a merge, (3) a split or (4) no relationship. Classification techniques used are described in (Parikh et al., 1997). Distance was defined as the city block distance, i.e., the sum of the absolute values of the row difference and the column difference. The number of values added into the sum increased as partial paths were extended from the beginning of the evolutionary process until the end of the seeding period.

The fitness of an individual was defined in terms of this sum of deviations from predictions. If there was no tracking event in the next image that was within range (as defined by the number of rows and columns that a storm system could move within the given time period) of a given tracking event and the corresponding value in a chromosome track indicated the existence of a track, the distance value for that part of the track was specified by a “not feasible penalty”. Similarly, there was a “premature end penalty” if the value in a chromosome track position was zero and there was in reality a good corresponding tracking event in the next image.

7. Discussion of results and concluding remarks

The sea level pressure tracks for two storm systems, STORM P and STORM A, that originated in the Pacific and Atlantic Oceans, respectively, close to 5 April 1989 are shown in Fig. 2 and the corresponding results for the cloud system tracks using our three different techniques are shown in Figs. 3–5. It is to be noted that the tracks for the k-nearest neighbor analysis and for the self-organizing maps were restarted manually a maximum of one time when the track was lost. The loss of a track is denoted in the figures by a break in the line segments of the track. The evolutionary sys-

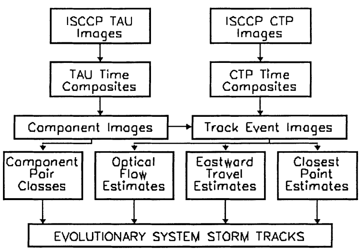

Fig. 1. Processing steps for storm tracking evolutionary system.

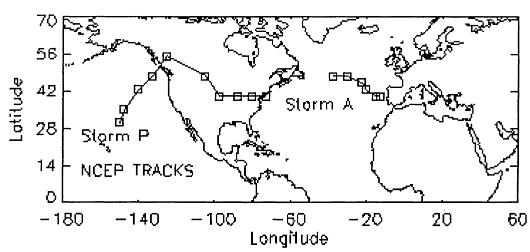

Fig. 2. NCEP sea level pressure tracks for storms P and A.

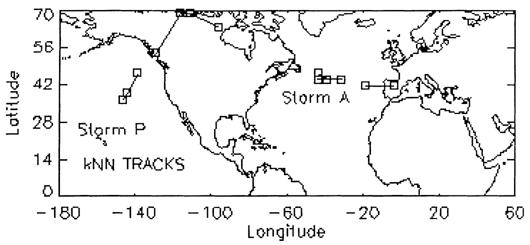

Fig. 3. k-Nearest neighbor cloud tracks for storms P and A.

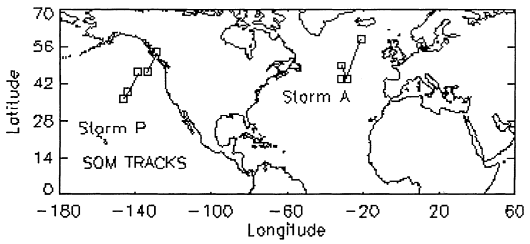

Fig. 4. Self-organizing map cloud tracks for storms P and A.

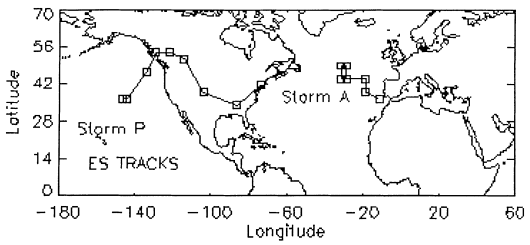

Fig. 5. Evolutionary system cloud tracks for storms P and A.

tem, however, was able to follow the track without any manual restart and also was able to investigate and output other feasible tracks. These capabilities represent potential advantages of evolutionary techniques for tracking storm systems over standard pattern classification techniques and data clustering techniques such as self-organizing maps. All three automatic techniques yielded results that were generally consistent with each other at locations where domain-specific knowledge or longer track look-ahead analyses were not necessary. The evolutionary system, which did have the ability to compare tracks throughout a long time period, produced not only complete tracking results but also results which were more consistent than the results produced by the correspondence-based techniques with the movement of the cloud systems associated with the low sea level pressure tracks.

Our evolutionary system is currently still under development. We have been investigating the addition of a smoothness term to the evaluation function that would not prohibit a storm system from turning sharply in response to factors such as location of the jet stream. We expect to add in future improved estimates of optical flow and information based on analyses of cloud system structures. A significant advantage of the evolutionary system framework is that it provides a mechanism for the incorporation of domain-specific expertise into the tracking procedure. The results of this study demonstrate the potential of evolutionary techniques for tracking synoptic-scale cloud systems associated with midlatitude storms through low resolution cloud product datasets. Future research will focus on enhancements to the system and application of the system to datasets from different months and years.

Discussion

Goode: You mentioned a couple of times that you were intending to include the information about cloud structure to enhance your tracking performance. How do you incorporate that information?

Parikh: The evaluation function in the evolutionary algorithm computes the sum of the distances between the next tracking event (as specified within an individual chromosome) and the best prediction of the next tracking event. During the initial seeding period, as partial tracks are extended, and also during the processing after the initial seeding period, the best prediction for the next tracking event is an event that lies within a corresponding cloud structure (for the lowest threshold level). At the previous Pattern Recognition in Practice conference, PRP-V, we presented a paper that discussed our methodology for classification of correspondences between cloud structures. (*Note of the editors*: *see Parikh et al.* (*1997*) *in this paper*).

Goode: Have you considered incorporating a probability distribution for different cloud structures and maybe a Bayesian approach?

Parikh: We are looking at only one type of cloud structure here: cloud structures that are very high and represent deep convective systems. We are thresholding these storm cloud structures into different categories defined by atmospheric scientists. Essentially, there is just only one cloud classification category, namely deep convective systems.

Acknowledgements

The authors would like to express their appreciation to William B. Rossow for his guidance and contributions to this research. The ISCCP D1 data sets which were used in this study originated at NASA Goddard Institute for Space Studies and were downloaded from the webserver at the NASA Langley Research Center EOSDIS Distributed Active Archive Center.

References

Anandan, P., 1989. A computational framework and an algorithm for the measurement of visual motion. Internat. J. Computer Vision 2, 283–301.

Arnaud, Y., Desbois, Y., Maizi, J., 1992. Automatic tracking and characterization of African convective systems on Meteosat pictures. J. Appl. Meteor. 31, 443–453.

Barron, R., Fleet, D.J., Beachemin, S.S., 1994. Performance of optical flow techniques. Internat. J. Comput. Vision 12 (1), 43–77.

Bolla, R., Marchese, M., Nobile, C., Zappatore, Z., 1997. Prediction of short-term evolution of cloud formations based on meteostat image sequences. In: Proc. ICIAP'95, pp. 677–682.

Carbonaro, A., Zingaretti, P., 1997. Object tracking in a varying environment. In: Proceedings of the Sixth International Conference on Image Processing and its Applications, pp. 229–223.

Endlich, R.M., Wolf, D.E., 1981. Automatic cloud tracking applied to goes and metostat observations. J. Appl. Meteor. 20 (3), 309–319.

Kohonen, T., Hynninen, J., Kangas, J., Laaksonen, J., 1995. SOM-PAK: The self-organizing map program package (Version 3.1).

Lane, D.M., Chantler, M.J., Dai, D., 1998. Robust tracking of multiple objects in sector-scan sonar image sequences using optial flow motion estimation. J. Oceanic Engrg. 23 (1).

Levine, D., 1996. Users Guide to the PGAPack Parallel Genetic Algorithm Library.

Parikh, J.A., DaPonte, J.S., Vitale, J.N., Tselioudis, G., 1997. Comparison of genetic algorithm systems with neural network and statistical techniques for analysis of cloud structures in midlatitude storm systems. Pattern Recognition Letters 18 (11–13), 1347–1351.

Parikh, J.A., DaPonte, J.S., Vitale, J.N., Tselioudis, G., 1998. Application of evoltionary technieques to temporal classification of cloud systems using satellite imagery. In: SPIE 3390, 69–76.

Parikh, J.A., DaPonte, J.S., Vitale, J.N., 1999. Unsupervised classification techniques for determination of storm region correspondences. In: Proc. SPIE 3722, 276–283.

Rossow, W.B., Schiffer, R.A., 1991. Isccp clooud data products. Bull. Am. Meteor. Soc. 72 (1), 2–20.

Silver, D., Wang, X., 1997. Tracking and visualising turbulent 3D features. IEEE Trans. Visualization and Computer Graphics 3 (2), 129–141.

Tselioudis, G., Zhang, Y., Rossow, W.B., 1999. Cloud and radiation variations associated with northern midlatitude low and high sea level pressure regimes. J. Climate (in press).

Voicu, L.I., Myler, H.R., 1998. Cloning operator and its applications. In: Proc. SPIE 3390, 57–68.

Wu, Q.X., 1995. A correlation-relaxation-labeling framework for computing optical flow – template matching from a new perspective. IEEE Trans. Pattern Anal. and Mach. Intell. 17 (8), 843–853.

Xiao, J., Michalewicz, Z., Zhang, L., 1997. Adaptive evolutionary planner/navigator for mobile robots. IEEE Trans. Evolution. Comput. 1 (1), 18–28.